Three-Dimensional Modeling of Earthquake Ground Motion Including Nonlinear Wave Propagation in Soils

Ricardo Taborda and Jacobo Bielak

Computational Seismology Laboratory, Department of Civil and Environmental Engineering, Carnegie Mellon University

Abstract

We present a study of the synthetic earthquake ground motion obtained in a three-dimensional model of a realistic basin, taking into consideration the nonlinear characteristics of the soil in the basin. In this initial analysis, nonlinearity is implemented by modeling the soil with the von Mises and Drucker-Prager formulation for elastoplastic materials. We simulate a hypothetical scenario earthquake, and solve the inelastic wave equations by means of the finite element spatial discretization method using an in-house developed octree-based parallel software for the simulation of ground motion due to earthquakes generated by kinematic faulting. The solution of the resulting semi-discrete nonlinear elastoplastic ordinary differential equations is computed explicitly step-by-step. The simulation is conducted on a parallel computer where each processor receives a portion of the unstructured mesh and computes the solution in an element-by-element fashion. We compare the results of the elastic and inelastic response of the basin. The comparison reveals the importance of considering nonlinear soil conditions and gives relevant insights about the influence of three-dimensionality for a problem that is often simplified into one- or two-dimensional models. Our work ultimately aims at fully incorporating nonlinearity into large-scale earthquake simulations, which to date do not yet consider this important aspect in three-dimensional strong ground motion modeling and analysis.

Case Study:
Euroseistest Numerical Benchmark

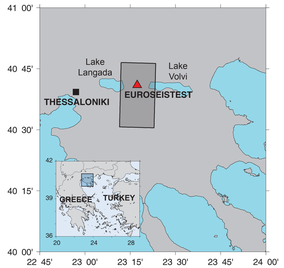

Figure 1. Location of the Euroseistest and horizontal projection of the modeling area.

In 2008 several research groups gathered to define a numerical benchmark to conduct different numerical simulations for the Euroseistest to thoroughly verify the different numerical methods on well-defined test cases (Bard et al., 2008). Phase I of this effort included a 3D simulation of an area of about 16 km x 29 km subjected to a hypothetical earthquake with epicenter just beneath the pass between the basins of the Volvi and Langada lakes in the Mygdonian graben. We build upon and modified the benchmark case to study the effect that nonlinear soil conditions may have in the response of the valley.

Figure 1 shows the region of Thessaloniki—an extensively studied, earthquake-prone region in nothern Greece—, the location of the Euroseistest, and the modeling area. The latter is shown in greater detail in Fig. 2, which also includes the location of the source and indicates two recording locations and three vertical cross sections of interest. These cross sections may be seen in Fig. 3. The original model used in the benchmark was based upon the information described in Pitilakis (2008) and consisted of three soft layers (with $Vs_{\min}$ = 200 m/s) on top of a horizontally layered bedrock with Vs values

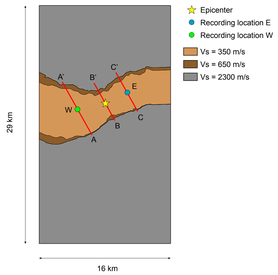

Figure 2. Location of observation points overlapped onto the shear wave velocity at the surface.

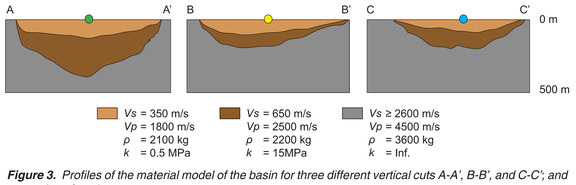

Figure 3. Profiles of the material model of the basin for three different vertical cuts A-A', B-B', and C-C'; and properties of each stratum.

starting at 2600 m/s at 500 m depth, and increasing with depth up to 4400 m/s at 39 m depth. Here, we have omitted the uppermost soft layer because of numerical modeling convenience.

The excitation is a point source located at 5 km depth, represented by a double couple that generates an earthquake of magnitude M_W = 5.3. The main characteristics of the source are shown in Table 1. Figure 4 shows the normalized slip, and the slip rate with its corresponding Fourier amplitude spectrum. This slip function is the same as that defined for the Euroseistest benchmark but has been refiltered at 1Hz (lowpass). The final slip and area of rupture have been appropriately scaled to generate the given magnitude.

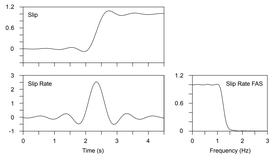

Figure 4. Source time functions (left) and spectrum of the slip rate (right). The slip is normalized with respect to the final slip.

Table 1. Location and mechanism of the double-couple point source. Depth is relative to sea level.

Long.	Lat.	Depth	Strike	Dip	Rake	$f_{\max}$	M_W
23°17'32''	40°39'52''	5 km	260°	40°	–90°	1.2 Hz	5.26

Modeling Elastoplastic Wave Propagation

During the last decade our research group has been part of multiple efforts within SCEC aimed at using a physics-based approach to seismic wave propagation problems through numerical modeling. We have developed a robust parallel software, named *Hercules*, that uses an unstructured octree-based finite element approach (Fig. 5) to solve the problem of anelastic wave propagation due to earthquakes generated by kinematic faulting, and successfully verified our implementation with others using different methods (Bielak et al., 2009).

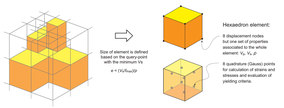

Figure 5. Hercules' unstructured mesh and typical hexahedron element with displacement nodes and stress/strain quadrature points.

Recently we have incorporated into *Hercules* the capability of considering nonlinear soil characteristics. For this purpose we have incorporated two material models of classical plasticity: von Mises and Drucker-Prager (Fig. 6). We have done so without substantially compromising *Hercules* performance by computing explicitly, step by step, the resulting semi-discrete nonlinear elastoplastic ordinary differential equations. We evaluate the yielding function at 8 quadrature points in each element and determine if a 'correction' due to plasticity is necessary to prevent a particle from crossing the yield surface.

For the particular case of the present simulation we have assumed the two upper layers to be cohesive-frictionless materials (von Mises model). The maximum strength, k of each stratum is shown in Fig. 3. The upper layer k was artificially lowered to force the occurrence of nonlinear behavior in the valley.

The simulation was done for a maximum frequency of 1 Hz. However, the mesh was built to be valid up to 2 Hz (6.7M elements). This allowed us to appropriately handle the appearance of higher frequencies due to the nonlinear soil. The simulation required 1.1 hours of computation using 8192 processors.

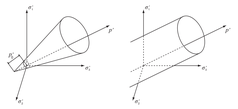

Figure 6. Drucker-Prager and von Mises yielding criteria in the principal stresses space.

Results and Analysis:

Regional level

Figure 7 shows a comparison between the elastic and elastoplastic response of the valley for the peak accumulated surface displacements and accelerations in a subset of the modeling area enclosing the region of interest. The effect of considering the upper soil layers as nonlinear is immediately noticeable. In the displacements we see an increase in the response of the East side of the valley, whereas the displacements seem to decrease in most of the West part of the region. The response in the immediate vicinity the epicenter also changes considerably.

A comparison of the accelerations evidences more dramatic changes. The appearance of higher frequencies due to nonlinearities increases the spatial variability of the motion; although there are reductions in the accelerations near the North edge of the valley, the South edge, especially Southwest from the epicenter, exhibits a considerable increase in the surface response.

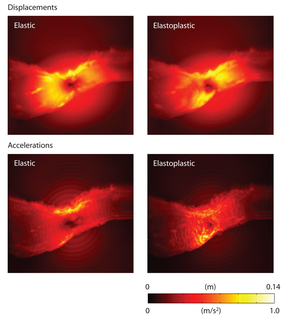

Figure 7. Peak accumulated surface displacements and accelerations computed as the square root of the sum of squares of the two horizontal components.

Local level

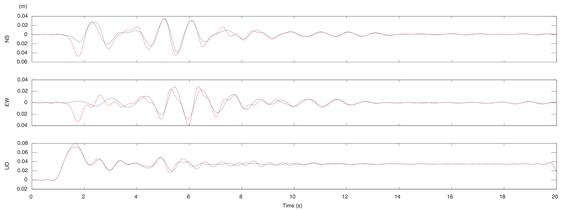

Figure 8. Displacement time histories at the epicenter. The blue traces correspond to the elastic case and the red ones to the elastoplastic case.

Figure 8 shows a comparison between the elastic and elastoplastic displacements at the epicenter. In this particular location, the effect of nonlinearity in the soil is most prominent for primary waves, during the initial stage of the ground motion, especially for the two horizontal components.

We have made alternative simulations placing the source away from the valley and closer to the surface, and have observed that this change in the location of the hypocenter has a strong effect on the relative elastic and inelastic ground motions; that is, in this case, the larger nonlinearities are associated with surfaces waves.

Element level

Figure 9 shows the horizontal shear stress-strain histories as implicit functions of time at three locations extracted from the finite elements at the free surface, both for the elastic and the elastoplastic cases. At all three points the bulk of the inelastic deformation occurred near the onset of the excitation. However, the detailed inelastic behavior is slightly different at each point. The element that contains the West observation point (see location of the three points in Fig. 2) experienced the smallest inelastic excursion and shows small permanent strains. In the element that contains the East observation point the inelastic deformation is two-sided, with greater hysteretic energy; yet, the permanent deformation in the two elements is similar. By contrast, the element that contains the epicenter experiences a much larger inelastic deformation than the other two elements. This deformation is responsible for the large inelastic displacements compared to the elastic ones observed near the beginning of the excitation in Fig. 8. Notice that very little nonlinear deformations occur thereafter in this element. Thus, the permanent deformation is large compared with that in the other two elements. Notice also the clear reduction in the maximum shear inelastic stresses with respect to the corresponding ones in the element above the epicenter. The other two elements experience smaller reductions.

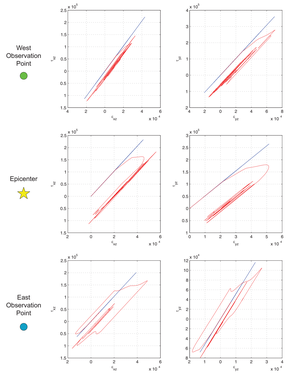

Figure 9. Stress-strain curves for three different locations (West, epicenter, and East) extracted from the finite element at the surface. Blue: elastic. Red: Elastoplastic.

Acknowledgment

This work was supported by the U.S. Geological Survey (USGS), Department of the Interior, under USGS award: Hybrid Three-Dimensional Modeling of Earthquake Ground Motion in Basins, Including Nonlinear Wave Propagation in Soils (08HQGR0018); and through NSF award: Toward Petascale Simulation of Urban Earthquake Impacts (NSF OCI-0749227). This research was also supported by an allocation of advanced computing resources supported by the National Science Foundation; and by an allocation through the TeraGrid Advanced Support Program. The computations were performed on BigBen at the Pittsburgh Supercomputing Center (PSC), and Kraken at the National Institute for Computational Sciences (NICS). The views and conclusions contained in this document are those of the authors and should not be interpreted as necessarily representing the official policies, either expressed or implied, of the U.S. Government.

References

Bard P.-Y., Chaljub E., Hollender F., Manakou M. and Pitilakis K. (2008), "Euroseistest Numerical Benchmark: Phase I", Commissariat à l'énergie atomique (CEC), Report distributed to the participants of the Cashima-Euroseistest Benchmark.

Bielak J., Graves R.W., Olsen K.B., Taborda R., Ramírez-Guzmán L., Day S.M., Ely G.P., Roten D., Jordan T.H., Maechling P.J., Urbanic J. and Juve G. (2009), "The ShakeOut earthquake Scenario: Verification of three simulation sets", Submitted for publication.

Pitilakis K. (2008), "EuroSeisTest report for the Cashima project", Technical report, Department of Civil Engineering, Aristotle University of Thessaloniki, Greece, Report distributed to the participants of the Cashima-Euroseistest Benchmark.